

# Compact Models for Double Gate MOSFET with Quantum Mechanical Effects Using Lambert Function

H. Abebe\*, E. Cumberbatch\*\*, H. Morris\*\* and V. Tyree\*

\*USC Viterbi School of Engineering, Information Sciences Institute, MOSIS service, Marina del Rey, CA 90292, USA. Tel: (310) 448-8740, Fax: (310) 823-5624, e-mail: [abebeh@mosis.com](mailto:abebeh@mosis.com) and [tyree@mosis.com](mailto:tyree@mosis.com)

\*\*Claremont Graduate University, School of Mathematical Sciences, 710 N College Ave, Claremont, CA 91711, USA. Tel: (909) 607-3369, Fax: (909) 621-8390, e-mail: [ellis.cumberbatch@cgu.edu](mailto:ellis.cumberbatch@cgu.edu) and [hedley.morris@cgu.edu](mailto:hedley.morris@cgu.edu)

## ABSTRACT

This paper is a continuation of the work presented in [5]. Iterative compact device models with quantum mechanical effects for a Double Gate (DG) MOSFET are presented using the Lambert function approach [4, 5]. The quantum model is based on the triangular potential and band gap widening approximations on the intrinsic electron density [1, 2]. The channel current model simulation results are shown in Figure 2-3 and in Figure 4 the charge and capacitance simulations are compared with the Schrödinger-Poisson one dimensional numerical results that are generated from SCHRED [6].

**Keywords:** device modeling, DG MOSFET, quantum effect, SPICE

## 1 INTRODUCTION

Taur and Lu, [3], have derived expressions for the I-V characteristics for DG MOSFET device which has the geometry shown in figure 1. The formula obtained in [3] requires the solution of a transcendental equation for an intermediate function  $\beta$ . In this paper this transcendental equation, (3), is solved iteratively with very fast convergence using the rational functions listed in the last section (see the Appendix). The work also includes quantum mechanical effects for nano-scale DG MOSFET.

An accurate model for quantum confinement effects in a nano-scale DG MOSFET device can be achieved by solving the coupled Schrödinger and Poisson equations using self-consistent numerical methods [1, 6]. However, some approximations must be made on the electrostatic potential near the silicon/oxide interface to get a compact analytical model. The approximations used for an analytical solution usually come in the form of triangular potential

well profile, with effective surface field [1, 2, 9]. The triangular potential approximation is used here for modeling the channel current and total gate capacitance.

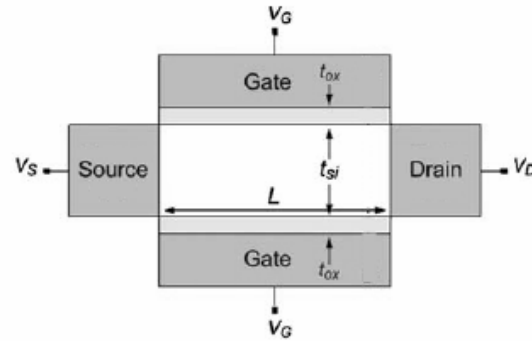


Figure 1. The structure of a double gate (DG) MOSFET

## 2 COMPACT DEVICE MODELS WITH QUANTUM MECHANICAL EFFECT

The channel current for undoped (or lightly doped) long channel DG MOSFET with very thin oxide is derived in [3] as

$$I_{ds} = I_{ds0} \left[ \beta \tan \beta - \frac{1}{2} \beta^2 + r \beta^2 \tan^2 \beta \right]_{\beta_s}^{\beta_D} \quad (1)$$

where  $I_{ds0} = \mu \frac{W}{L} \frac{4\epsilon_{si}}{t_{si}} \left( \frac{2kT}{q} \right)^2$ ,  $r = \frac{\epsilon_{si} t_{ox}}{\epsilon_{ox} t_{si}}$  and  $\beta$  is a

solution of the equation

$$\ln(\beta \sec \beta) + 2r\beta \tan \beta = \nu$$

$$\nu = \frac{q(V_g - \Delta\phi - V)}{2kT} - \ln\left(\frac{2}{t_{si}} \sqrt{\frac{2\epsilon_{si} kT}{q^2 n_i}}\right) \quad (2)$$

The electron density is  $n = n_i e^{(\psi - V)/V_{th}}$ . The total mobile charge per unit gate area is given by  $Q = 2\epsilon_{si} (d\psi/dx)_{x=t_{si}/2} = 2\epsilon_{si} (2kT/q)(2\beta/t_{si}) \tan\beta$ .

The parameters:

$q$  represents electron charge.

$\psi$  electrostatic potential.

$\epsilon_{si}$  semiconductor permittivity.

$\epsilon_{ox}$  silicon-oxide permittivity.

$t_{si}$  silicon thickness.

$t_{ox}$  oxide thickness.

$n_i$  intrinsic density.

$V_g$  the gate voltage.

$V_{th} = kT/q$  thermal voltage.

$k$  Boltzmann constant.

$T$  temperature.

$V$  quasi-Fermi potential, where  $V=0$  at the source and  $V=V_{ds}$  at the drain.

Equation (2) can be recast into the form

$$(2rz)e^{2rz} = x \quad (3)$$

where  $z = \beta \tan \beta$  and  $x = (2r \sin \beta)e^v$

The solution of the above equation (3) is

$$z = \frac{1}{2r} \text{LambertW}(x) \quad (4)$$

From (3) and (4) we can write

$$\beta = \Phi\left[\frac{1}{2r} \text{LambertW}(x)\right] \quad (5)$$

where  $\Phi(z)$  is the solution of the equation  $z = \Phi \tan \Phi$  and  $\text{LambertW}(x)$  function is the solution of  $x = We^W$  (see [7]). As  $0 \leq \beta \leq \pi/2$  the argument of  $\text{LambertW}(x)$  remains positive. Accurate approximations for  $\text{LambertW}(x)$  and the function  $\Phi(z)$  are given in the Appendix. An iterative solution can easily be found to equation (5) by using the low voltage approximation as an initial solution to  $\beta$ . To determine the low voltage solution it is necessary to rewrite (3) as

$$\beta e^{-v} = e^{-2r\beta \tan \beta} \cos \beta \quad (6)$$

The right hand side of (6) has the Taylor expansion

$$e^{-2r\beta \tan \beta} \cos \beta = 1 - \left(\frac{4r+1}{2}\right)\beta^2 + O(\beta^4) \quad (7)$$

Equations (6) and (7) give a quadratic in  $\beta$  and by means of the quadratic formula we can get the recursion

$$\beta_{(n+1)} = \Phi\left[\frac{1}{2r} \text{LambertW}(2r \sin \beta_n e^v)\right] \quad (8)$$

where  $n=0, 1, 2 \dots$  with the initial estimate

$$\beta_0 = \frac{e^{-v}}{(4r+1)} (-1 + \sqrt{1 + 2(4r+1)e^{2v}}). \text{ Using only}$$

four iterations one obtains excellent results compared to the numerical (see figures 2 and 3).

**Quantum effect:** One of the reasons that most of the modern silicon MOSFETs are fabricated on <100> oriented substrates is due to the smallest interface-trap density compared to <111> and <110> crystal plane orientations. In this section <100> silicon orientation is considered. The quantum effect near the silicon/oxide interface can be described by solving the 1D Schrödinger equations (for the longitudinal effective mass and again for the transverse effective mass). However, more than 90% of the electrons are concentrated in the ground state and the remaining less than 10% are in the first excited state. The computation that determines the charge density is simplified by considering the Schrödinger equation only along the longitudinal direction

$$\frac{d^2\psi_j}{dx^2} + \frac{2m^*}{\hbar^2} [E_j - U]\psi_j = 0 \quad (9)$$

where  $\psi_j$  is the electron wave function with the corresponding energy eigenvalue  $E_j$ ,  $\hbar$  is Planck's constant divided by  $2\pi$ ,  $m^* = 0.916m_e$  is electron effective mass in the direction perpendicular to the transistor channel surface and  $m_e$  is the free electron mass. The boundary conditions for the wave function used in this work are:  $\psi_j(x=0) = \psi_j(x \rightarrow \infty) = 0$ .

The band bending near the silicon/oxide interface at strong inversion confines the carriers to a narrow surface channel and an electron in the semiconductor conduction band is bounded and its energy is quantized. A constant density of states assumption and the Fermi-Dirac statistics give the electron concentration in  $j^{\text{th}}$  sub-band as

$$N_j = \frac{0.38m_e}{\pi\hbar^2} \int_{E_j}^{\infty} \frac{dE}{1 + e^{(E-E_f)/kT}} = \quad (10)$$

$$0.38m_e \left(\frac{kT}{\pi\hbar^2}\right) \ln(1 + e^{(E_f-E_j)/kT})$$

where  $j=0, 1, 2 \dots$ ,  $E_f$  is the Fermi energy,

Substituting the triangular well approximation for  $U$  in (9) and solving the eigenvalue problem gives the **Airy functions** as solutions for the Schrödinger equation with energy eigenvalue

$$E_j = \left(\frac{\hbar^2}{2m^*}\right)^{1/3} \left((3/2)\pi q F_s \left(j + \frac{3}{4}\right)\right)^{2/3} \quad (11)$$

where  $F_s$  is the surface electric field.

It is also possible to get a similar analytical expression to (11) using the Wentzel-Kramer-Brillouin (WKB) method of asymptotic approximation (see [8]).

Stern, [1], pointed out that (11) is a good approximation when the MOS device is at depletion but overestimates the ground state eigenvalues at strong inversion by 6% compared to the numerical result. In [9] it is shown that replacing  $F_s$  by the effective surface field  $F_{seff}$  using the weighting coefficient can significantly improve the accuracy of (11) at strong inversion.

The classical description of the semiconductor intrinsic density is

$$n_i^c = 2 \left( \frac{kT}{2\pi\hbar^2} \right)^{\frac{3}{2}} (m_h m_e)^{\frac{3}{4}} e^{-E_g/2kT} \quad (12)$$

where  $E_g$  is the semiconductor energy gap and  $m_h$  is mass of the hole.

As a result of the quantum confinement effect near the interface, the semiconductor band gap will increase by  $\Delta E_g$  and this increase can be estimated from the energy difference of the electron ground state and the edge of conduction band, [2, 10]:

$$\Delta E_g = \frac{13}{9} \beta^* (\epsilon_{si} / 4kT)^{1/3} (F_{seff})^{2/3} \quad (13)$$

where  $\beta^* = 6.6 \times 10^{-29} J \cdot m$ ,  $F_{seff} = \eta(V_g + V_t) / t_{ox}$ , the threshold voltage  $V_t = V_{t0} + 2V_{th} \ln[q(V_g - V_{t0}) / 4rkT]$ ,  $V_{t0} = \Delta\phi + 2V_{th} \ln\left[\frac{2}{t_{si}} \sqrt{2\epsilon_{si} kT / q^2 n_i^c}\right]$  and the weighting coefficient  $\eta=0.5$ .

The quantum correction for the intrinsic density becomes

$$n_i^q = e^{-\Delta E_g / 2kT} n_i^c \quad (14)$$

### 3 RESULTS AND DISCUSSIONS

In this section we present comparisons of our simulation results with the numerical and SCHRED. The simulation results in figures 2-4 are generated using (1), (8) and (14). The compact iteration approach gives excellent results compared to the exact numerical for  $L=W$  square device (see figures 2 and 3). In figure 4 our quantum confinement simulation results give good comparison with the self-consistent Schrödinger-Poisson numerical results, SCHRED. The compact quantum simulation results, dash lines, show a significant reduction of the channel current and gate capacitance from the classical simulations, which are the solid lines.

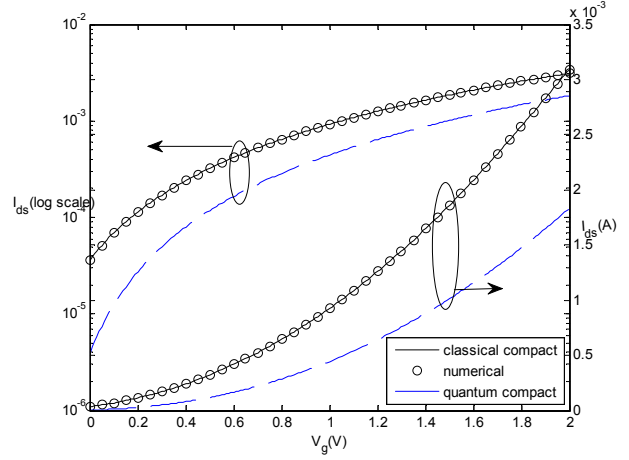


Figure 2: Channel current versus gate voltage for  $V_{ds}=2V$ ,  $\Delta\phi = -0.75V$ ,  $\mu = 300 \text{ cm}^2 / V \cdot s$ , DG MOSFET with 5nm silicon and 1.5nm oxide thicknesses.

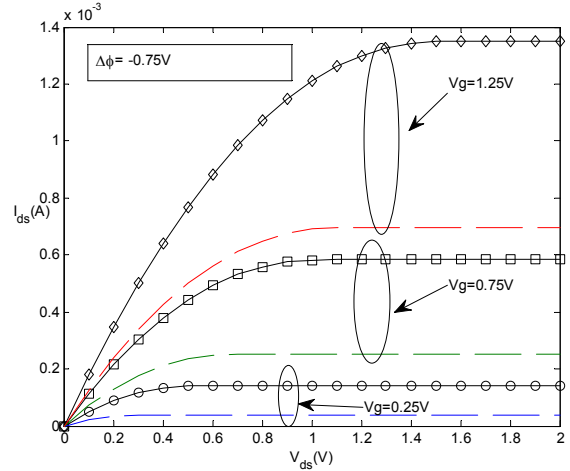


Figure 3: Channel current versus source-drain voltage for  $\mu = 300 \text{ cm}^2 / V \cdot s$ , DG MOSFET with 5nm silicon and 1.5nm oxide thicknesses.

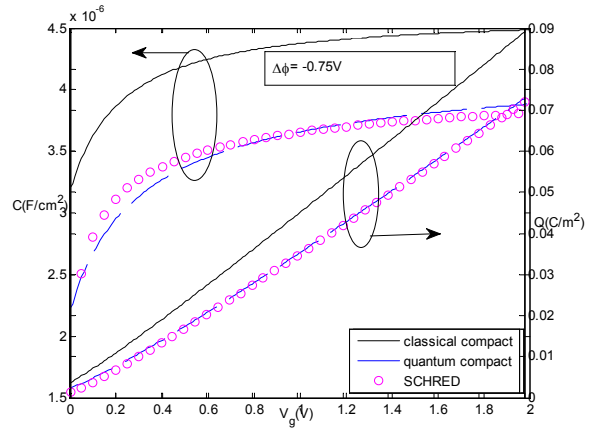


Figure 4: Total mobile charge and gate capacitance versus gate voltage plots for  $\mu = 300 \text{ cm}^2 / V \cdot s$ , DG MOSFET with 5nm silicon and 1.5nm oxide thicknesses.

## REFERENCES

- [1] M. Stern, "Self-consistent result for n-type Si inversion layers." *Physical Review B*, vol. 5, No. 12, pp. 4891-4899, 15 June (1972).
- [2] M. J. Van Dort, P. H. Woerlee and A. J. Walker, "A simple model for quantization effects in heavily-doped silicon MOSFETs at inversion conditions," *Solid State Electronics*, Vol. 37, No. 3, pp. 411-414, (1994).
- [3] H. Lu and Y. Taur, "Physics-Based, Non-Charge-Sheet Compact Modeling of Double Gate MOSFETs," *Nanotech Proceedings, WCM*, pp. 58-62, May 8-12, (2005), Anaheim, CA.
- [4] A. Ortiz-Conde, F. J. Garcia Sanchez, M. Guzman, "Exact Analytical Solution of Channel Surface Potential as an Explicit Function of Gate Voltage in Undoped-body MOSFETs Using the Lambert  $W$  function and a Threshold Voltage Definition," *Solid-State Electronics*, Vol. 47, No. 11, pp. 2067-2074, (2003).
- [5] H. Morris, E. Cumberbatch, H. Abebe and V. Tyree, "Compact modeling for the I-V characteristics of double gate and surround gate MOSFETs," *IEEE UGIM Proceedings*, pp. 117-121, June 25-28, (2006), San Jose, CA.
- [6] SCHRED, <http://www.nanohub.org>
- [7] R. Corless, G. Gonnet, D. Hare, D. Jeffrey, and D. Knuth, "On the Lambert  $W$  function", *Advances in Computational Mathematics* 5(4): 329-359 (1996).
- [8] H. Abebe, E. Cumberbatch, H. Morris and V. Tyree, "Analytical models for quantized sub-band energy levels and inversion charge centroid for MOS structures derived from asymptotic and WKB approximations," *Proceedings 2006 Nanotechnology Conference*, Vol. 3, pp. 519-522, May 7-11, (2006), Boston, Massachusetts, USA.
- [9] Yutao Ma, Litian Liu, Zhiping Yu, and Zhijian Li, "Validity and applicability of triangular potential well approximation in modeling of MOS structure inversion and accumulation layers," *IEEE Trans. on Electron Devices*, Vol. 47, No. 9, September (2000).
- [10] Zhiping Yu, Robert W. Dutton, and Richard A. Kiehl, "Circuit/Device modeling at the quantum level," *IEEE, Computational Electronics, Six international workshop on July* (1998), pp. 222-229.

## APPENDIX

### I. Approximation of the function $\Phi(z)$ :

The function  $\Phi(z)$  is the solution of the equation  $\Phi \tan \Phi = z$  and  $\tan \Phi$  can be approximated by the rational expression

$$\tan \Phi \cong \frac{\Phi_0 + \left(\frac{1}{3} - \gamma\right)\Phi_0^3}{1 - \gamma\Phi_0^2 + \delta\Phi_0^4}$$

$$\text{where } \gamma = \frac{40}{9\pi^2} \text{ and } \delta = \frac{16}{9\pi^4}$$

Using the above rational expression, the first approximation of  $\Phi(z)$  becomes

$$\Phi_0 = \sqrt{\frac{(1+z\gamma) - \sqrt{(z\gamma-1)^2 - 4z(z\delta-1/3)}}{2(z\delta+\gamma-1/3)}}$$

The first order Taylor expansion near  $z_0 = \Phi_0 \tan \Phi_0$  gives

$$\Phi(z) = \Phi_0 - \frac{(\Phi_0 \tan \Phi_0 - z)}{\tan \Phi_0 + \Phi_0 \sec^2 \Phi_0}$$

### II. Approximation of the Lambert $W(x)$ function

The following rational functions are given in [7] for Lambert  $W$  function approximation:

$$y = z - \frac{z(z-1)}{1+z} + \frac{z(z-1)^2}{2(1+z)^3} - \frac{(z-1)^3(z-2z^2)}{6(1+z)^5} + \frac{z(6z^2-8z+1)(z-1)^4}{24(1+z)^7} - \frac{z(24z^3-58z^2+22z-1)(z-1)^5}{120(1+z)^9} + \frac{z(120z^4-444z^3+328z^2-52z+1)}{720(1+z)^{11}} - \frac{z(720z^5-3708z^4+4400z^3-1452z^2+114z-1)}{5040(1+z)^{13}}$$

with  $z = x/e$ , provides a good approximation to Lambert $W(x)$  for  $x < 8$  and the function

$$y = L_1 - L_2 + \frac{L_2}{L_1} + \frac{L_2(-2+L_2)}{2L_1^2} + \frac{L_2(6-9L_2+2L_2^2)}{6L_1^3} + \frac{L_2(-12+36L_2-22L_2^2+3L_2^3)}{12L_1^4} + \frac{L_2(60-300L_2+350L_2^2-125L_2^3+12L_2^4)}{60L_1^5}$$

with  $L_1 = \ln(x)$  and  $L_2 = \ln \ln(x)$ , is a good approximation to Lambert $W(x)$  for  $x \geq 8$ . These two formulae together provide a good compact formula for Lambert $W(x)$  over the entire positive domain.